Turkish Journal of Electrical Engineering & Computer Sciences

http://journals.tubitak.gov.tr/elektrik/

Research Article

Turk J Elec Eng & Comp Sci
(2014) 22: 1354 – 1366

doi:10.3906/elk-1212-75

A new approach of nonblind watermarking methods based on DWT and SVD via LU decomposition

Onur JANE*, Ersin ELBAŞI
The Scientific and Technological Research Council of Turkey (TÜBİTAK), Kavaklıdere, Ankara, Turkey

Received: 14.12.2012 • **Accepted:** 25.01.2013 • **Published Online:** 15.08.2014 • **Printed:** 12.09.2014

Abstract: Multimedia security has been the focal point of considerable research activity in the last decade, mainly because of its wide application area. Watermarking, in particular, is identified as a major technology to achieve copyright protection and multimedia security. Therefore, recent studies in the literature include some evident approaches for embedding data into a multimedia element. Because of its useful frequency component separation, the discrete wavelet transform (DWT) is commonly used in watermarking schemes. Moreover, singular value decomposition (SVD) and lower-and-upper (LU) decomposition have little effect on the perception of the watermark. Therefore, in this study, a combination of DWT and SVD via LU decomposition is proposed as a new nonblind watermarking algorithm that requires cover work to detect the watermark. Experimental results show that the proposed algorithm is considerably robust and reliable against certain attacks without degrading the input image, by embedding a binary watermark on the low-low band. Moreover, the threshold values are data-dependent for watermarks after attacks; that is, the threshold value is always different from another for certain attacks so that similarity ratios in this algorithm, as a quality metric, are much more than those of the other algorithms consisting of DWT and/or SVD despite strong attacks causing lower peak signal-to-noise ratio values. Apart from robustness, reliability, and data-dependence, the other novel aspect of this study is to expand the application areas of watermarking with a new algorithm consisting of DWT, LU, and SVD, and this study will contribute to the literature for certain cases.

Key words: Multimedia security, digital image watermarking, discrete wavelet transform, singular value decomposition, lower and upper decomposition, peak signal-to-noise ratio, similarity ratio, nonblind watermarking

1. Introduction

Multimedia security has been the focal point of considerable research activity in the last decade, mainly because of its wide application area. Digital watermarking, in particular, is the process that embeds data called a watermark into a multimedia object (such as text, audio, image, and video), such that the watermark can be detected or extracted later to make an assertion about the object [1]. Apart from copy control and copyright protection, broadcast monitoring, fingerprinting, indexing, medical applications, and content authentication are other application areas of digital watermarking. For the purpose of designing and developing a new watermarking algorithm in those application areas, the most important properties are robustness and invisibility [2], which are the main points of this study.

There are basically 2 approaches to embed a watermark: spatial domain and transform domain watermarking. In the spatial domain, the watermark is embedded by modifying the pixel values in the original image. The simplest spatial domain watermarking technique is to embed the bits of the message directly into the least

*Correspondence: onur.jane@tubitak.gov.tr

significant bit plane of the cover image [3]. Transform domain watermarking is similar to spatial domain watermarking; in this case, the coefficients of transforms such as discrete cosine transform (DCT), discrete Fourier transform (DFT), or discrete wavelet transform (DWT) are modified [4].

Watermark detection is classified into 3 categories: nonblind, blind, and semiblind watermarking. Nonblind watermarking requires the original image to detect the watermark, the blind technique does not require the original image to detect the watermark, and the semiblind watermarking technique requires the watermarked document for detection.

In this study, visual, invisible, and nonblind binary watermarking is embedded into the cover image in the transform domain. The rest of this paper is organized as follows. Section 2 reviews related studies on spatial and transform domain watermarking in the literature. Watermark embedding and extraction algorithms are explained in detail in Sections 3 and 4, respectively. Section 5 illustrates the experimental results, and, finally, Section 6 concludes this work.

2. Related works

The principle of transform domain watermarking techniques is to modify transform coefficients with an appropriate algorithm. In this study, a novel watermarking algorithm with the combination of DWT and singular value decomposition (SVD) via lower-and-upper (LU) decomposition will be implemented. Therefore, previous studies in the literature are discussed in the following text.

a) Discrete wavelet transform (DWT): Due to its great frequency component separation properties, the DWT, in contrast to the DCT, is very useful to identify the coefficients to be watermarked [5]. The DWT separates an image into a lower resolution image [low-low (LL)] and horizontal [high-low (HL)], vertical [low-high (LH)], and diagonal [high-high (HH)] detail components. The magnitudes of the DWT coefficients are larger in the LL bands at each level of decomposition. Embedding the watermark in higher level subbands increases the robustness of the watermark. However, the image visual fidelity may be lost, which can be measured by the peak signal-to-noise ratio (PSNR). With the DWT, the edges and texture can be easily identified in the high-frequency bands, HH, LH, and HL. The large coefficients in these bands normally indicate edges in the image. Therefore, the DWT understands the human visual system better in comparison to the DCT.

Dugad et al. [5] proposed a wavelet-based scheme for watermarking images by embedding the watermark into the LL band coefficients in the same way as Cox et al. had previously proposed [6]. Hsieh and Tseng proposed a DWT-based algorithm in the following steps: an original image was decomposed into wavelet coefficients. Next, a multienergy watermarking scheme, based on the qualified significant wavelet tree, was used to achieve a robust algorithm [7]. Elbasi and Eskicioglu embedded a pseudorandom sequence as a watermark in 2 bands (LL and HH) using DWT [8]. After that study, Elbaşı proposed a novel video watermarking system based on the hidden Markov model (HMM), which split the video sequences into a group of pictures (GOP) and then embedded portions of the binary into each GOP with a wavelet domain watermarking algorithm in the LL and HH subbands [9].

In general, most of the image energy is concentrated at the lower frequency coefficient set of LL bands, and therefore embedding watermarks in these coefficient sets may degrade the image significantly. However, embedding the watermark in the LL bands effectively increases robustness [10]. One fact that makes our study novel is that we increase the robustness of the watermarked image under certain attacks without degrading the image, by embedding a binary watermark on the LL band. This also explains why the LL subband is chosen for watermark embedding.

b) Singular value decomposition (SVD): Any m $\times$ n matrix A can be factored into $A = U \times S \times V^T$ (orthogonal) (diagonal) (orthogonal). The columns of U (m $\times$ m) (left singular vectors) are eigenvectors of $A \times A^T$ and the columns of V (n $\times$ n) (right singular vectors) are eigenvectors of $A^T \times A$ [11]. The U and V matrices are orthogonal matrices, so that $U^T \times U = I$ and $V^T \times V = I$, where I is the unit matrix. Columns of the U and V matrices are called left and right singular vectors, which represent horizontal and vertical details of an image, respectively [12]. Their singular values on the diagonal of S (m $\times$ n) are the square roots of the nonzero eigenvalues of both $A \times A^T$ and $A^T \times A$. If A is an image, in this case, S, the diagonal matrix with rank R, has the luminance (gray-scale) values of the image layers produced by U and V.

Gorodetski et al. proposed an approach on embedding some data through slight modifications of singular values of a small block of the segmented covers [13]. Chandra divided the image into subblocks, applied SVD to those blocks, and modified their largest singular value by a watermark and a scaling factor [14]. Liu and Ran used a pseudo-Gaussian random number as a watermark and added it to the singular values of the original image [15]. Calagna et al. divided the cover image into blocks and applied SVD to each block. In order to balance the embedding capacity with distortion, the watermark was embedded in all of the nonzero singular values according to the local features of the cover image [16] in that study. Bao and Ma proposed an image-adaptive watermarking scheme for image authentication by applying a simple quantization-index-modulation process on wavelet domain SVD [17]. Ghazy et al. designed a new watermarking algorithm in the following order: the original image was divided into blocks, and then the watermark was embedded in the singular values of each block separately. Watermark detection was implemented by extracting the watermark from the singular values of the watermarked blocks [18].

c) LU decomposition: Any square matrix A can be written as a product of the L and U matrices. LU decomposition for the example of a 3 $\times$ 3 matrix is shown in Eq. (1).

$$A = L \times U = \begin{bmatrix} 1 & 0 & 0 \\ l_{21} & 1 & 0 \\ l_{31} & l_{32} & 1 \end{bmatrix} \times \begin{bmatrix} d_1 & u_{12} & u_{13} \\ 0 & d_2 & u_{23} \\ 0 & 0 & d_3 \end{bmatrix} \tag{1}$$

As seen in Eq. (1), the matrix L is lower triangular, with 1s on the diagonal and the multipliers below the diagonal [11]. U, on the other hand, is upper triangular, with some coefficients on the diagonal and the multipliers above the diagonal. The LU form is not symmetric in this case; the L always has 1s on the diagonal, whereas U does not. Therefore, in this study, we will divide out of U a diagonal matrix D, which is made up entirely of the d_n coefficients, as shown in Eq. (2).

$$A = L \times D \times U = \begin{bmatrix} 1 & 0 & 0 \\ l_{21} & 1 & 0 \\ l_{31} & l_{32} & 1 \end{bmatrix} \times \begin{bmatrix} d_1 & 0 & 0 \\ 0 & d_2 & 0 \\ 0 & 0 & d_3 \end{bmatrix} \times \begin{bmatrix} 1 & u_{12}/d_1 & u_{13}/d_1 \\ 0 & 1 & u_{23}/d_2 \\ 0 & 0 & 1 \end{bmatrix} \tag{2}$$

Niu et al. transformed the corresponding nonnegative matrix of the image into a G-diagonally dominant matrix in order to apply LU decomposition with DCT midfrequency coefficients as a blind watermarking [19]. Wang et al. transformed the input image into the wavelet domain using DWT, computed the variances of the last details, and selected detail matrix information among subbands whose variance is the maximum one. Next, they decomposed the preprocessed image into LU factorization and embedded the watermark into the nonzero pixels of 2 triangular matrixes adaptively [20].

There are very few studies of LU decomposition in watermarking applications. Therefore, the other novel aspect of this study is to expand the application areas of watermarking with a new algorithm that will be helpful in the literature for certain cases.

Measurement of image and video quality is a challenging problem in a wide range of applications [21,22]. The quality measures can be classified into 2 groups: subjective and objective. There are a number of objective measures. We mention some of these measures below.

a) Mean squared error (MSE): This is an old, proven measure of control and quality. The MSE is defined as in Eq. (3):

$$MSE = \frac{1}{M \times N} \sum_i \sum_j \left[A\left(i,j\right) - Aw(i,j)\right]^2, \tag{3}$$

where $A(i,j)$ is the original image and $Aw(i,j)$ is the watermarked image, both of which contain $M \times N$ pixels.

b) PSNR: This is most commonly used as a measure of quality of reconstruction in image watermarking. It is a ratio between the maximum value of a signal and the magnitude of background noise [23]. It is most easily defined via the MSE for an 8-bit gray-scale image, as shown in Eq. (4).

$$PSNR = 20 \times log\left(\frac{255}{\sqrt{MSE}}\right) \tag{4}$$

c) Similarity ratio (SR): This is defined as in Eq. (5):

$$SR = \frac{S}{S + D}, \tag{5}$$

where S and D represent the number of matching pixel values in compared images and the number of different pixel values in compared images, respectively. The SR is used in evaluation of nonblind watermark extraction. Moreover, the SR provides high precision for binary image watermarks. When different pixel values converge to 0, the SR will be close to 1, which is the optimum and desired condition.

3. Watermark embedding algorithm

In our proposed study, the watermark embedding procedure is as follows.

Input: Cover work (A) and binary image watermark (W)

Output: Watermarked image (AW)

1. Using DWT, decompose the cover work, A, into 4 subbands: LL, LH, HL, and HH.
2. Decompose the LL band into LU factorization with its components L, D, and U, as in Eq. (2): $LL = L \times D \times U$.
3. Apply SVD to D: $D = (UDw) \times (SDw) \times \left(VDw^T\right)$.
4. Apply SVD to W: $W = (Uw) \times (Sw) \times \left(Vw^T\right)$.
5. Modify SDw, the singular values of the D component, by adding the singular values of the watermark, W, with the scaling factor α: $Dw = SDw + \alpha \times Sw$.

6. Since the singular value of the watermark image is directly added to the singular values of D with the scaling factor, it is wise to reconstruct D by updated coefficient Dw: $Dww = (UDw) \times (Dw) \times \left(VDw^T\right)$.
7. Because the diagonal matrix (D) of the LL subband is updated, it is time to gather L, Dww, and U to obtain LL1w: $LL1w = L \times Dww \times U$.
8. Compute the inverse DWT to obtain the watermarked cover image, AW.
9. Store the locations of the 1s in W in order to use them as a key in the extraction algorithm.

A flow diagram of the watermark embedding algorithm is shown in Figure 1.

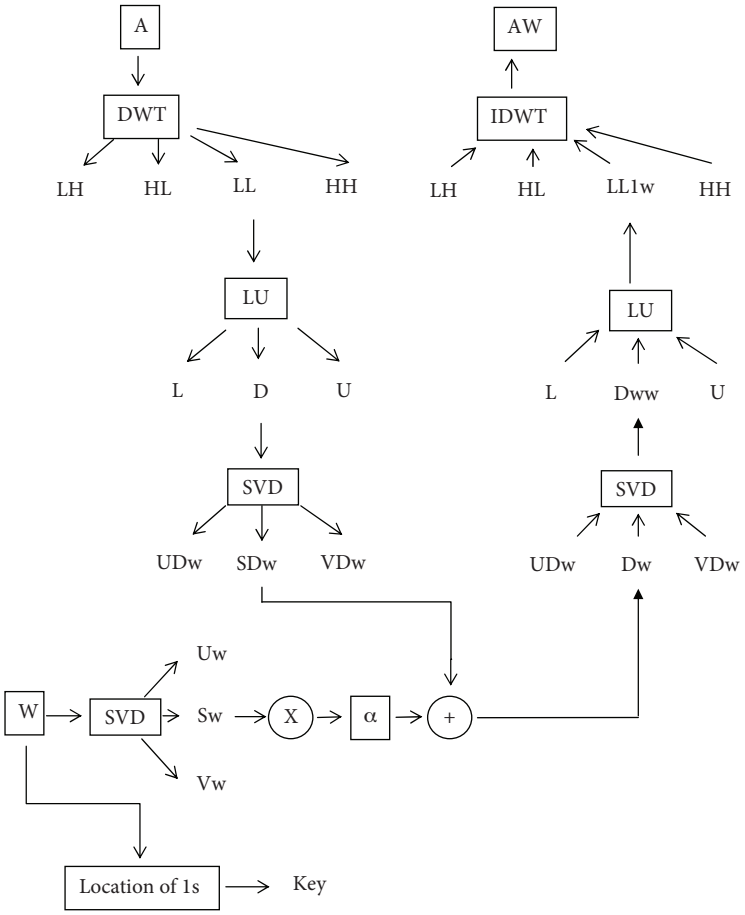

Figure 1. Flow diagram of the watermark embedding algorithm.

4. Watermark extraction algorithm

According to the watermark embedding algorithm in the previous section, the watermark extraction procedure is as follows.

Input: Attacked watermarked image (AW*)

Output: Extracted watermark (W*)

1. Using DWT, decompose the watermarked and possibly attacked image, AW*, into 4 subbands: LLw, LHw, HLw, and HHw.

2. Decompose LLw into LU factorization with its components L*, D*, and U*, as in Eq. (2): $LLw = (L^*) \times (D^*) \times (U^*)$.

3. Apply SVD to D*: $D^* = (UDw^*) \times (SDw^*) \times (VDw^*)$.

4. Extract the singular values of the watermark Sw*: $Sw^* = \frac{(SDw^* - SDw)}{\alpha}$.

5. Extract the watermark with its SVD components: $W^* = (Uw) \times (Sw^*) \times \left(Vw^T\right)$.

6. Use the key, which is the location of the pixels stored in the embedding algorithm. If the mean value of the pixels in the key (TH) for W* is positive, assign that pixel value to binary 0, or otherwise to binary 1.

A flow diagram of the watermark extraction algorithm is shown in Figure 2.

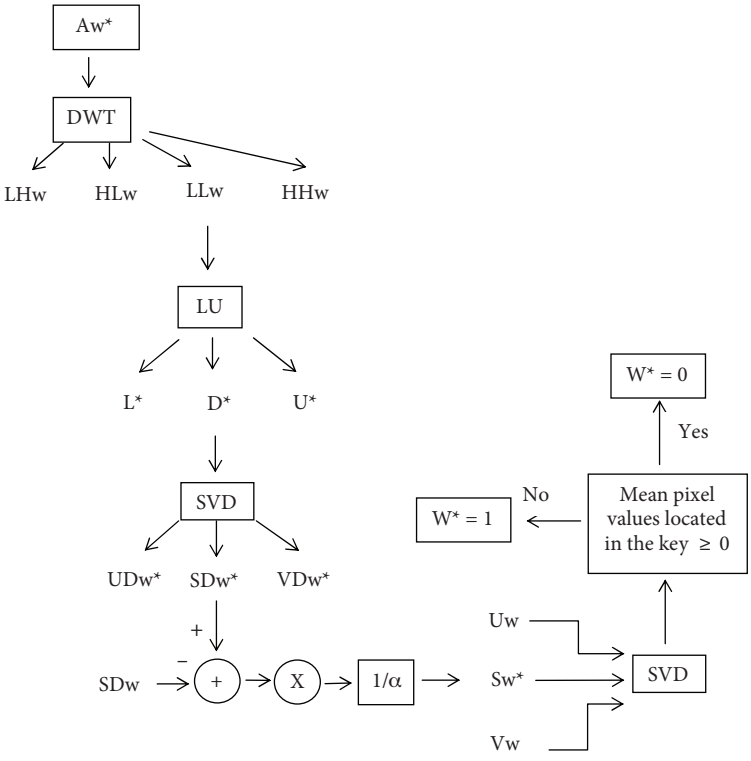

Figure 2. Flow diagram of the watermark extraction algorithm.

5. Experimental results

Images used in this proposed watermarking algorithm are shown in Figure 3. Baboon and Cameraman in Figures 3a and 3b, respectively are 8-bit 512 × 512 gray-scale images. Figure 3c shows the 256 × 256 watermark used as a binary image.

In order to obtain good visual quality of watermarked images, choosing a scaling factor value, α, plays an important role in watermark embedding procedures [24]. If the value of α is chosen close to 0, the watermarked image is less distorted and the maximum PSNR can be obtained. However, for lower α values, watermarked images are less robust to several attacks, which means a lower SR. Therefore, while choosing the optimum value

of α, it is useful in practice to investigate the PSNR values of extracted watermark images after several attacks and to make a trade-off analysis of them.

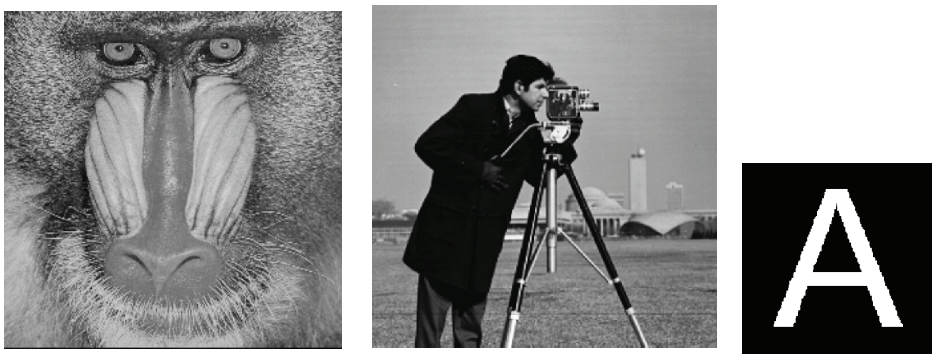

a b c

Figure 3. a) Baboon, b) Cameraman, and c) watermark.

Guiding the selection of the optimum scaling factor in the watermark embedding algorithm for 'filtering', 'scaling', and 'rotation' attacks, Table 1 shows the changes in the PSNR values for α at certain intervals for the cover work in Figure 3a.

In the same manner, Table 2 shows the changes in the PSNR values for scaling factors at certain intervals for the cover work in Figure 3b.

After investigating Tables 1 and 2 in detail, it is seen that the maximum PSNR values for several attacks are not helpful for choosing the optimum scaling factor values for both Baboon and Cameraman. Watermark embedding and extraction algorithms are complements of each other. Thus, it is worthwhile to investigate extracted watermarks with their SR values. Related columns in Tables 1 and 2 show the changes in the SR values for scaling factors at certain intervals for both Baboon and Cameraman, respectively. Even though the PSNR values after some attacks are too low to extract the watermark from them, our proposed algorithm provides a SR high enough, close to 1.0. Since the PSNR and SR values in Tables 1 and 2 should be evaluated as a whole in the concept of embedding and extracting, respectively, a trade-off analysis between the PSNR and SR for both cover works in Figure 3 helps to choose the optimum scaling factor as 1.1, which is also consistent among attacks.

Figure 4 shows watermarked images after using related scaling factors and applying the watermark embedding algorithm in Section 3.

Accepting that PSNR values between 30 and 40 dB be considered as satisfactory, the experimental results show that the watermark embedding algorithm is successful enough to use in several applications. Nevertheless, the watermark embedding and extraction algorithms should be evaluated together. Thus, it is worthwhile to investigate extracted watermarks after the predefined attacks shown in both Tables 1 and 2.

Figure 5 shows watermarked Baboon images and their PSNR values after attacks.

In a similar way, Figure 6 shows watermarked Cameraman images and their PSNR values after attacks.

Figure 7 shows extracted watermark images from attacked Baboon with the calculated SR and TH values after applying the watermark extraction algorithm from Section 4.

Table 1. Variations of the PSNR and SR values on different scaling factors and attacks for Baboon.

Baboon	Filtering (low-pass)		Scaling (512 × 512 → 256 × 256, down-sampling)		Rotation (20°)	
Scaling factor	PSNR (dB)	SR	PSNR (dB)	SR	PSNR (dB)	SR
0.1	23.26014	0.88588	22.5189	0.88237	11.55146	0.756866
0.3	23.25637	0.882156	22.5166	0.881256	11.55067	0.150131
0.5	23.24817	0.88121	22.51127	0.880646	11.54948	0.199509
0.7	23.23549	0.883759	22.50346	0.881516	11.54786	0,243805
0.9	23.21834	0.881271	22.49227	0.881683	11.54584	0.866516
1.1	23.19711	0.88652	22.47915	0.874741	11.5434	0.897064
1.3	23.17206	0.878479	22.46204	0.881943	11.54056	0.209274
1.5	23.14225	0.878784	22.44209	0.879883	11.5373	0.88591
1.7	23.10837	0.880524	22.41983	0.881317	11.53363	0.182602
1.9	23.07047	0.884155	22.39528	0.879333	11.52955	0.860352

Table 2. Variations of the PSNR and SR values on different scaling factors and attacks for Cameraman.

Baboon	Filtering (low-pass)		Scaling (512 × 512 → 256 × 256, down-sampling)		Rotation (20°)	
Scaling factor	PSNR (dB)	SR	PSNR (dB)	SR	PSNR (dB)	SR
0.1	32.43664	0.894684	31.21904	0.890823	10.45683	0.800217
0.3	32.40758	0.898468	31.19476	0.889297	10.45498	0.808365
0.5	32.33528	0.88942	31.12295	0.890335	10.4528	0.773376
0.7	32.22893	0.897842	31.03356	0.890259	10.45029	0.831467
0.9	32.07889	0.895721	30.93216	0.889572	10.44744	0.807739
1.1	31.89586	0.898804	30.80346	0.890121	10.44426	0.743561
1.3	31.66836	0.897659	30.63084	0.890121	10.44074	0.776749
1.5	31.42983	0.895386	30.45672	0.88974	10.4369	0.807907
1.7	31.17723	0.898392	30.27242	0.889832	10.43272	0.773911
1.9	30.90462	0.891571	30.07026	0.889786	10.42822	0.710922

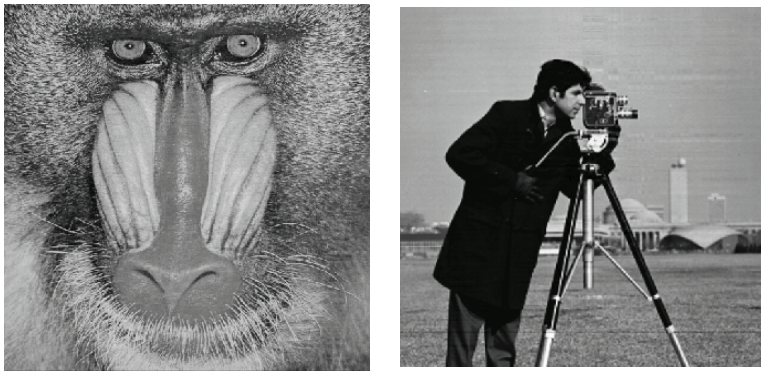

a b

Figure 4. a) Watermarked image, Baboon (α = 1.1; PSNR = 38.82 dB) and b) watermarked image, Cameraman (α = 1.1, PSNR = 39.13 dB).

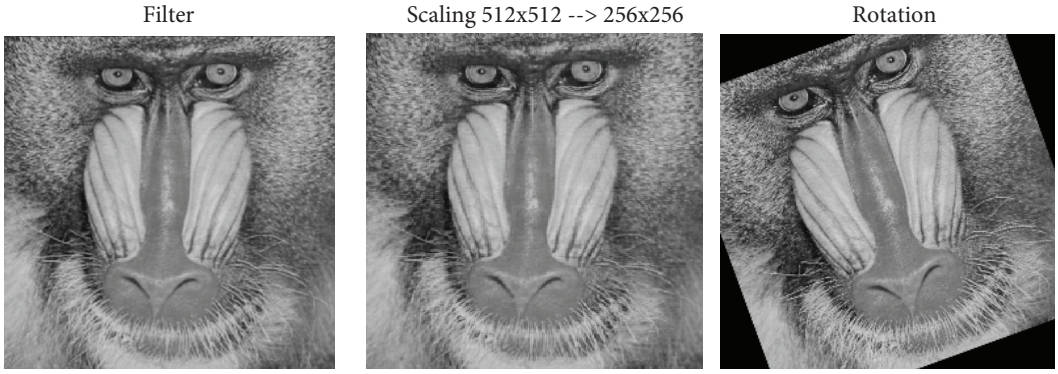

Figure 5. a) Filtering (23.20 dB), b) scaling 512 × 512 → 256 × 256 (22.48 dB), and c) rotation (11.54 dB).

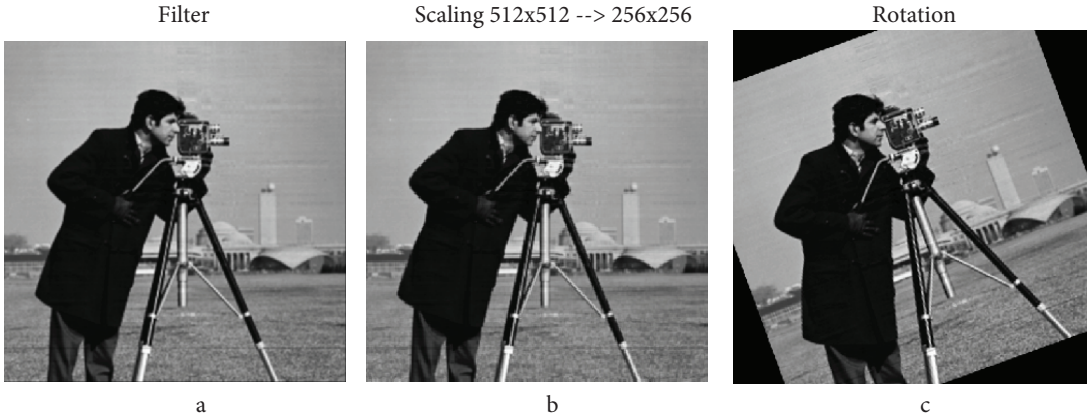

Figure 6. a) Filtering (31.90 dB), b) scaling 512 × 512 → 256 × 256 (30.80 dB), and c) rotation (10.44 dB).

In the same way, Figure 8 shows extracted watermark images from attacked Cameraman with calculated SR and TH values after applying the watermark extraction algorithm in Section 4.

The proposed algorithm is also applied to Lena as another cover work. In order to avoid displaying too many images in this paper, Table 3 gives clues about the experimental results for that test image.

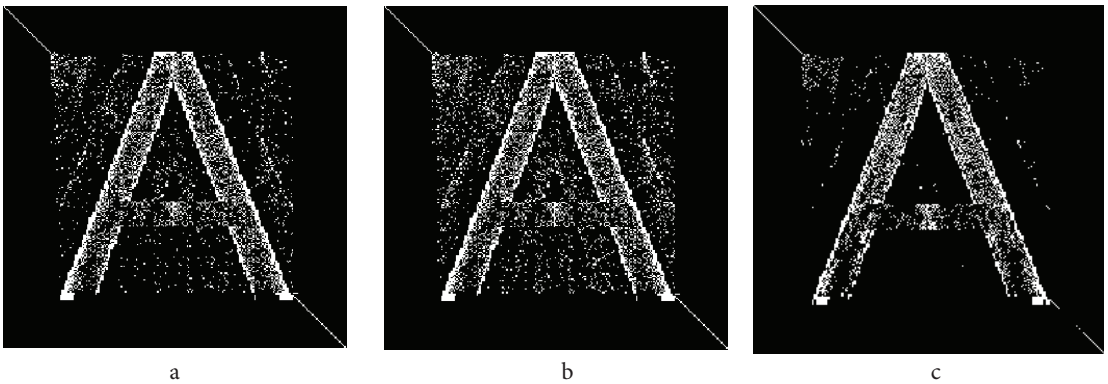

Figure 7. Extracted watermarks from attacked Baboon image with their SR and TH values: a) filtering (SR = 0.8865, TH = –12.12), b) scaling 512 × 512 → 256 × 256 (SR = 0.8747, TH = –12.62), and c) rotation (SR = 0.8971, TH = –3.28).

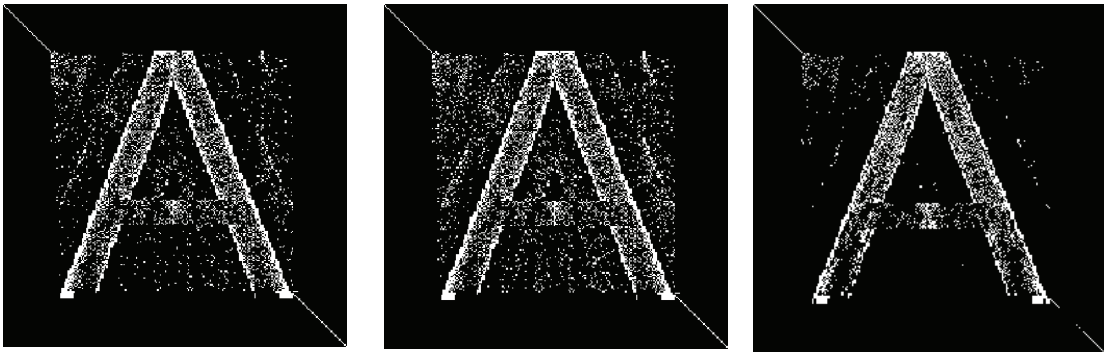

a b c

Figure 8. Extracted watermarks from attacked Cameraman image with their SR and TH values: a) filtering (SR = 0.8988, TH = –9.21), b) scaling 512 × 512 → 256 × 256 (SR = 0.8901, TH = –10.75), and c) rotation (SR = 0.7436, TH = –1.56).

Table 3. Experimental results for Lena.

Lena (α = 1.1, PSNR before attacks = 34.3301 dB)		
Attacks/control parameters	PSNR (dB)	SR
Filtering (low-pass)	30.5122	0.8828
Scaling (512 × 512 → 256 × 256, down sampling)	30.2031	0.8854
Rotation (20°)	11.1849	0.8815

6. Conclusion

This paper presents a novel approach in nonblind watermarking based on the combination of the DWT and SVD via LU decomposition. After decomposing the cover image into 4 subbands (LL, HL, LH, and HH), we decompose the LL band again into LU factorization with its L, D, and U matrices and apply SVD to the D component. Afterwards, we modify the diagonal singular value coefficients of D with the diagonal singular value coefficients of the watermark itself, W, using a scaling factor. The LL band coefficients are then reconstructed with modified singular values and D components, and finally the inverse DWT is applied to obtain the watermarked image.

Table 4 shows the SR and PSNR values before and after attacks for the algorithms based on DWT and/or SVD and the combination of DWT, LU, and SVD, as in this study.

According to Table 4, although the PSNR values for LU + DWT + SVD are less than those values for DWT and DWT + SVD, it does not prevent us from choosing the algorithm proposed in this study, because PSNR values between 30 and 40 dB are considered satisfactory for watermarking algorithms in the literature. In addition, PSNR values after attacks for all of the algorithms are very close; therefore, it is not necessary to take them into consideration as a decisive variable. Thus far, embedding control parameters have been discussed. As seen in Table 4, SR values in LU + DWT + SVD, which are used in extraction control parameters as a quality metric, are not only close to 1, but are also much greater than the values in the other algorithms, despite strong attacks causing lower PSNR values.

In our study, the frequently preferred transform domain technique DWT and decomposition method SVD are combined via LU decomposition so that watermarked images are much more robust against certain attacks. Thus, contrary to traditional DWT and SVD watermarking techniques, this proposed algorithm can be considered as robust against 'filtering', which represents compression-based attacks, and 'scaling' and 'rotation', which signify geometric attacks. This is because the change in the diagonal coefficients in the singular value

matrix in the SVD and diagonal decomposition matrix in the LU for the LL subband obtained by the DWT has little effect on the perception of the watermark.

Table 4. Comparative study of the SR, PSNR, and PSNR after attacks for different watermarking algorithms.

Cover works	Attacks	Control parameters	Watermarking algorithms		
			DWT	DWT + SVD	LU + DWT + SVD
Baboon	Filtering	SR	0.5354	0.8641	0.8865
		PSNR (dB)	61.36	82.17	38.82
		PSNR after attack (dB)	23.29	23.26	23.20
	Scaling	SR	0.5027	0.6473	0.8747
		PSNR (dB)	61.36	82.17	38.82
		PSNR after attack (dB)	22.52	22.52	22.48
	Rotation	SR	0.5524	0.9834	0.8971
		PSNR (dB)	61.36	82.18	38.82
		PSNR after attack (dB)	11.55	11.55	11.54
Cameraman	Filtering	SR	0.6992	0.8556	0.8988
		PSNR (dB)	61.36	81.39	39.13
		PSNR after attack (dB)	32.42	32.44	31.90
	Scaling	SR	0.5583	0.6053	0.8901
		PSNR (dB)	61.36	81.39	39.13
		PSNR after attack (dB)	31.20	31.22	30.80
	Rotation	SR	0.5950	0.9805	0.7436
		PSNR (dB)	61.36	81.39	39.13
		PSNR after attack (dB)	10.46	10.46	10.44
Lena	Filtering	SR	0.6343	0.8472	0.8828
		PSNR (dB)	61.36	81.50	34.33
		PSNR after attack (dB)	31.90	31.92	30.51
	Scaling	SR	0.5383	0.7002	0.8854
		PSNR (dB)	61.36	81.50	34.33
		PSNR after attack (dB)	31.35	31.38	30.20
	Rotation	SR	0.5740	0.9804	0.8815
		PSNR (dB)	61.36	81.50	34.33
		PSNR after attack (dB)	11.20	11.21	11.19

One fact that makes our study novel is that we increase robustness of the watermarked image under certain attacks without degrading the image by embedding a binary watermark on the LL band. This is why the LL subband is chosen. Another novel aspect of this study is to make an optimization analysis and decide on the scaling factor used in embedding and the threshold value used in extraction experimentally. In particular, threshold values are data-dependent for watermark data after attacks; therefore, threshold values are always different from one another for certain attacks. Finally, the other novel aspect of this study is to expand the application areas of watermarking with a new algorithm consisting of DWT, LU, and SVD. Consequently, this study will be helpful in the literature for certain cases.

Future works will be focused on more successful values of the SR for rotation and robustness against various attacks for the algorithm based on DWT and SVD via LU decomposition.

References

[1] S.P. Mohanty, N. Ranganathan, R.K. Namballa, "VLSI implementation of invisible digital watermarking algorithms towards the development of a secure JPEG encoder", Proceedings of the IEEE Workshop on Signal Processing System, pp. 183–188, 2003.

[2] C. Cruz-Ramos, R. Reyes-Reyes, M. Nakano-Miyatake, H. Perez-Meana, "A blind video watermarking scheme robust to frame attacks combined with MPEG2 compression", Journal of Applied Research and Technology, Vol. 8, pp. 323–369, 2010.

[3] F. Akar, Y. Yalman, H.S. Varol, "Data hiding in digital images using a partial optimization technique based on classical LSB method", Turkish Journal of Electrical Engineering & Computer Sciences, Vol. 21, pp. 2037–2047, 2012.

[4] Q. Zhang, Y. Li, X. Wei, "An improved robust and adaptive watermarking algorithm based on DCT", Journal of Applied Research and Technology, Vol. 10, pp. 405–415, 2012.

[5] R. Dugad, K. Ratakonda, N. Ahuja, "A new wavelet-based scheme for watermarking images", Proceedings of the 1998 International Conference on Image Processing, Vol. 2, pp. 419–423, 1998.

[6] I.J. Cox, J. Kilian, F.T. Leighton, T. Shamoon, "Secure spread spectrum watermarking for multimedia", IEEE Transactions on Image Processing, Vol. 6, pp. 1673–1687, 1997.

[7] M.S. Hsieh, D.C. Tseng, "Hiding digital watermarks using multiresolution wavelet transform", IEEE Transactions on Industrial Electronics, Vol. 48, pp. 875–882, 2001.

[8] E. Elbasi, A.M. Eskicioglu, "A DWT-based robust semi-blind image watermarking algorithm using two bands", Proceedings of the SPIE 18th Annual Symposium on Electronic Image Security, Steganography, and Watermarking of Multimedia Contents VIII, Vol. 6072, pp. 1–11, 2006.

[9] E. Elbaşı, "Robust multimedia watermarking: hidden Markov model approach for video sequences", Turkish Journal of Electrical Engineering & Computer Sciences, Vol. 18, pp. 159–170, 2010.

[10] S.P. Singh, P. Rawat, S. Agrawal, "A robust watermarking approach using DCT-DWT", International Journal of Emerging Technology and Advanced Engineering, Vol. 2, pp. 300–305, 2012.

[11] G. Strang, Linear Algebra and Its Applications, Stamford, CT, USA, The Thomson Corporation, 2005.

[12] E. Yavuz, Z. Telatar, "Improved SVD-DWT based digital image watermarking against watermark ambiguity", Proceedings of the 2007 ACM Symposium on Applied Computing, pp. 1051–1055, 2007.

[13] V.I. Gorodetski, L.J. Popyack, V. Samoilov, V.A. Skormin, "SVD-based approach to transparent embedding data into digital images", Proceedings of the International Workshop on Mathematical Methods, Models and Architectures for Computer Network Security, Vol. 2052, pp. 263–274, 2011.

[14] D.V.S. Chandra, "Digital image watermarking using singular value decomposition", Proceedings of the 45th Midwest Symposium on Circuits and Systems, Vol. 3, pp. 264–267, 2002.

[15] R. Liu, T. Tan, "An SVD-based watermarking scheme for protecting rightful ownership", IEEE Transactions on Multimedia, Vol. 4, pp. 121–128, 2002.

[16] M. Calagna, H. Guo, L.V. Mancini, S. Jajodia, "A robust watermarking system based on SVD compression", Proceedings of ACM Symposium on Applied Computing, pp. 1341–1347, 2006.

[17] P. Bao, X. Ma, "Image adaptive watermarking using wavelet domain singular value decomposition", IEEE Transactions on Circuits and Systems for Video Technology, Vol. 15, pp. 96–102, 2005.

[18] R.A. Ghazy, N.A. El-Fishawy, M.M. Hadhoud, M.I. Dessouky, F.E.A. El-Samie, "An efficient block-by-block SVD-based image watermarking scheme", Ubiquitous Computing and Communication Journal, Vol. 2, pp. 1–9, 2007.

[19] S.Z. Niu, X.X. Niu, Y.X. Yang, "Digital watermarking algorithm based on LU decomposition", Journal of Electronics & Information Technology, Vol. 26, pp. 1620–1625, 2004.

[20] S. Wang, W. Zhao, Z. Wang, "A gray scale watermarking algorithm based on LU factorization", International Symposiums on Information Processing, pp. 598–602, 2008.

[21] E. Elbasi, "A survey on digital image & video watermarking", First Portion of Second Examination Report, Graduate Center, The City University of New York, 2006.

[22] E. Elbasi, "Multimedia security: digital image and video watermarking", PhD, The City University of New York, 2007.

[23] Y. Yalman, İ. Ertürk, "A new color image quality measure based on YUV transformation and PSNR for human vision system", Turkish Journal of Electrical Engineering & Computer Sciences, Vol. 21, pp. 603–612, 2013.

[24] M. Jiang, "A new adaptive visible watermarking algorithm for document images", Information Technology Journal, Vol. 11, pp. 1322–1326, 2012.